Journal of Research of the National Bureau of Standards—D. Radio Propagation
Vol. 63D, No. 3, November–December 1959

Radio-Refractive-Index Climate Near the Ground

B. R. Bean and J. D. Horn

(February 6, 1959)

The radio refractive index of air is a function of atmospheric pressure, temperature, and humidity and is found to vary in a systematic fashion with climate. It was found that the surface value of the refractive index may be estimated four to five times more accurately from charts of reduced-to-sea-level values than from similar sized charts of surface index. Worldwide maps of 5-year means of this reduced value are presented for the months of February and August, for the minimum monthly mean value of the year and for the range of monthly mean values. Year-to-year variation of monthly means is also considered. Applications of these data to the prediction of radio field strengths indicate a possible 30-decibel difference in median level of identically equipped tropospheric communications systems due to climate alone.

1. Introduction

The radio refractive index of air, n, is a function of atmospheric pressure, temperature and humidity, thus combining in one parameter, three of the normal meteorological elements used to specify climate. In the following sections we will examine the variability of n during different seasons of the year and in differing climatic regions. The systematic dependence of n upon station elevation will make it necessary to consider a method of expressing n in terms of an equivalent sea-level value in order to see more clearly the actual climatic differences of the various parts of the world. After a consideration of the n climate of the world, the application of this information to such practical problems as the prediction of radio field strength and the refraction of radio waves will be discussed.

2. Presentation of Basic Data

Near the surface of the earth, for vhf and uhf frequencies, n is a number of the order of 1.0003. Since, for air, n never exceeds unity by more than a few parts in 10^{-4}, it is convenient to consider the climatic variation of n in terms of

$$N=(n-1)10^6=\frac{77.6}{T}\left(P+\frac{4810e_sRH}{T}\right), \qquad (1)$$

where P is the total atmospheric station pressure in millibars (mb), RH is the relative humidity in percent, and e_s the saturation vapor pressure in mb at the temperature, T, in deg Kelvin. The values of the constants in (1) were determined [1] [1] from a consideration of recent microwave and optical determinations of the refractive index of air and are considered to be accurate to 0.5 percent in N for frequencies up to 30,000 Mc in the ranges of temperature, pressure and humidity normally encountered. The notation N_s is used to indicate that (1) has been evaluated from standard surface weather observations.

To obtain long-term average values of N one should properly average individual observations over many years. This is difficult to do since, in general, only summaries of weather observations are readily available. However, long-term average values of temperature, pressure and humidity are available and may be converted into an "average" value of N. This "average" N differs from the true average since the intercorrelation of pressure, temperature, and humidity is neglected. This difference was examined by an analysis of 2 yr of weather records of the months of February and August at an arctic location (Fairbanks, Alaska), a temperate zone location (Washington, D.C.), and a tropical location (Swan Island, W.I.). These data, given in table 1, indicate that the difference between the two methods was never more than 1.5 N units and the average difference was less than 1 N unit which is small compared to commonly observed seasonal and geographic variations of 20 to 100 N units.

TABLE 1. *Two-year average value of* N_s *versus the value of* N_s *calculated from average temperature, pressure, and humidity*

	$\overline{N_s}$	$\overline{N_s}(\overline{P},\overline{T},\overline{RH})$	$\overline{N_s}-\overline{N_s}(\overline{P},\overline{T},\overline{RH})$
Fairbanks:			
February	314.0	313.0	1.0
August	320.5	320.0	0.5
Washington:			
February	305.5	304.5	1.0
August	356.0	354.5	1.5
Swan Island:			
February	362.0	362.5	0.5
August	387.5	388.0	.5
Average			0.83

[1] Figures in brackets indicate the literature references at the end of this paper.

On this basis it was decided to use the long term means given in the United Nations' monthly publication, *Climatic Data for the World*. This publication is particularly advantageous for our present study since it reports the fictitious value of the relative humidity needed to obtain the actual average vapor pressure from the saturated vapor pressure of the reported mean temperature [2].

Data from 306 weather stations were obtained in order to give reasonable geographical coverage. In general, 5 yr of record were obtained for each station from the period 1949 to 1958, preference being given to the years 1954 through 1958. A noticeable exception, however, was Russia for which only 1 yr of data (IGY) is reported in *Climatic Data for the World* and thus all charts are drawn with dashed contours for Russia. There are vast expanses of ocean for which there are no meteorological observing stations. Climatic atlases were utilized in order to present estimates of world climate in these locales. A reasonable coverage of the sparse data areas of the world was made by estimating temperature from sea surface isotherms [3] and humidity from charts of seasonal average depression of the wet bulb temperature [4]. Pressure was estimated for these locations from average winter and summer pressure charts.

When these data were converted to N [5] and charts prepared, a pronounced altitude dependence could be seen as in figure 1. Figure 1 plus the following charts of N variations across the United States are from an extensive N climatology now being prepared at the Central Radio Propagation Laboratory. Although the present study is primarily aimed toward worldwide variations, it is felt that the U.S. data better illustrate the height dependence of N_s and the subsequent reduction process employed. It is noted that the coastal areas display high values of N_s while the inland areas have lower values. There are low values of N_s corresponding to the Appalachian and Adirondack Mountains, a decrease with increasing elevation of the Great Plains until the lowest values are observed in the Rocky Mountain region and the high plateau area of Nevada. A corresponding gradient is observed from the West Coast eastward. Crosshatching encloses areas where the terrain changes so rapidly that it was felt the data were inadequate to obtain realistic contours of N_s.

The altitude dependence of N can be studied in terms of the "dry" and "wet" components of N. The dry term, D,

$$D=\frac{77.6P}{T}, \tag{2}$$

is proportional to air density and normally constitutes at least 60 percent of N.

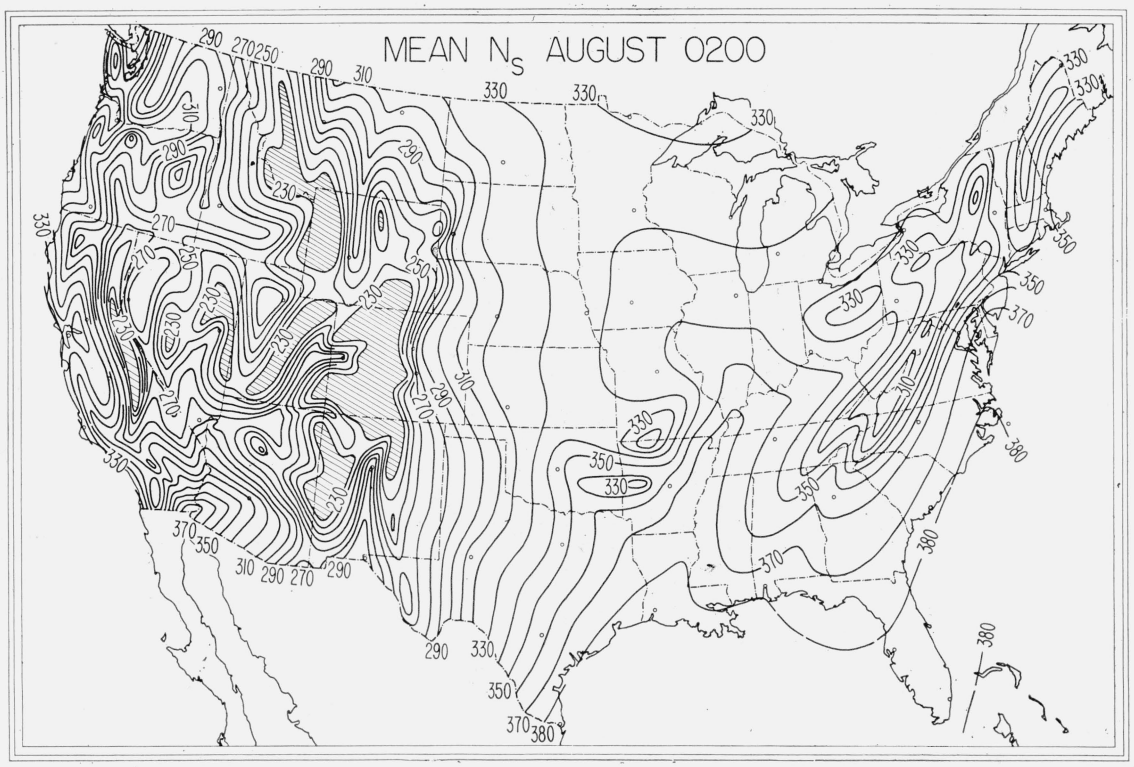

FIGURE 1. *Mean N_s, August 0200 local time.*

One would expect, from the hydrostatic equation in [6], that D would be an exponential function of height. Examination of D at the earth's surface versus station elevation shows this to be in fact true. By assuming an exponential decay between the value of N at sea level and 8 km the height coefficient of -0.1057/km was determined from the NACA dry standard atmosphere [7] and was adopted for general use. Thus, the station value, D_s, may be reduced to a sea-level value, D_0, by the relationship

$$D_0 = D_s \exp\{0.1057\, h\}, \tag{3}$$

where h is in kilometers. Values of D_0 obtained in this fashion as shown on figure 2 present a gradient that is remarkably free of detail compared to the N_s chart and is easily drawn for all areas of the country.

A similar investigation was made of the height dependence of the surface "wet" term, W_s, evaluated from

$$W = \frac{3.73 \times 10^5 e_s RH}{T^2}. \tag{4}$$

All the cases examined displayed low correlations of log W_s and height, indicating that W_s is not a marked exponential function of height. Thus W_s is plotted alone as on figure 3. Again, contours of W_s may be obtained easily for all sections of the country.

At this point in the reduction process there are two maps, one of D_0 and one of W_s. A further simplification is accomplished by introducing the approximation of reducing N_s by the dry term height correction to obtain a single reduced value, N_0;

$$N_0 = (D_s + W_s) \exp\{0.1057\, h\}. \tag{5}$$

Figure 4 gives the N_0 contours for the same time as the previous maps of D_0 and W_s. The N_0 maps are no more difficult to prepare than the W_s maps and have effectively removed the station height dependence of N_s. One might wonder at the advisability of arbitrarily reducing the wet term by the dry term correction. For the coastal areas of the country, where the exponential height correction factor is nearly one, this amounts simply to adding the D_0 and W_s maps while for the mountain areas, where the height correction factor is large, the W_s values are small with the result that the gradient of the N isopleths obtained from the D_0 and W_s maps is essentially maintained on the N_0 maps. As an example, for the series of maps under discussion, the $(D_0 + W_s)$ difference between Reno, Nev. (1,340-m elevation) and Oakland, Calif. (5.5-m elevation) is 21 N units, while the N_0 difference is 19 N units.

The effects of this correction on the worldwide values can be seen from figure 5 where N_s is plotted versus station elevation in km. A sample line illus-

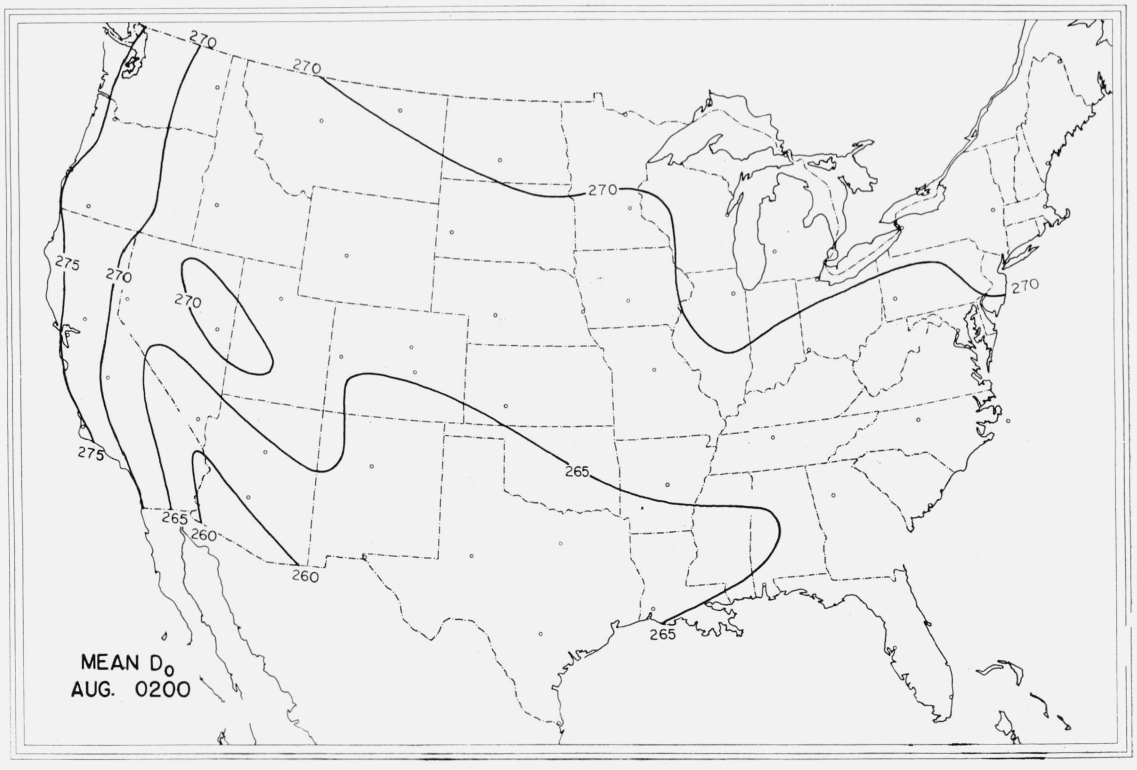

FIGURE 2. *Mean D_o, August 0200 local time.*

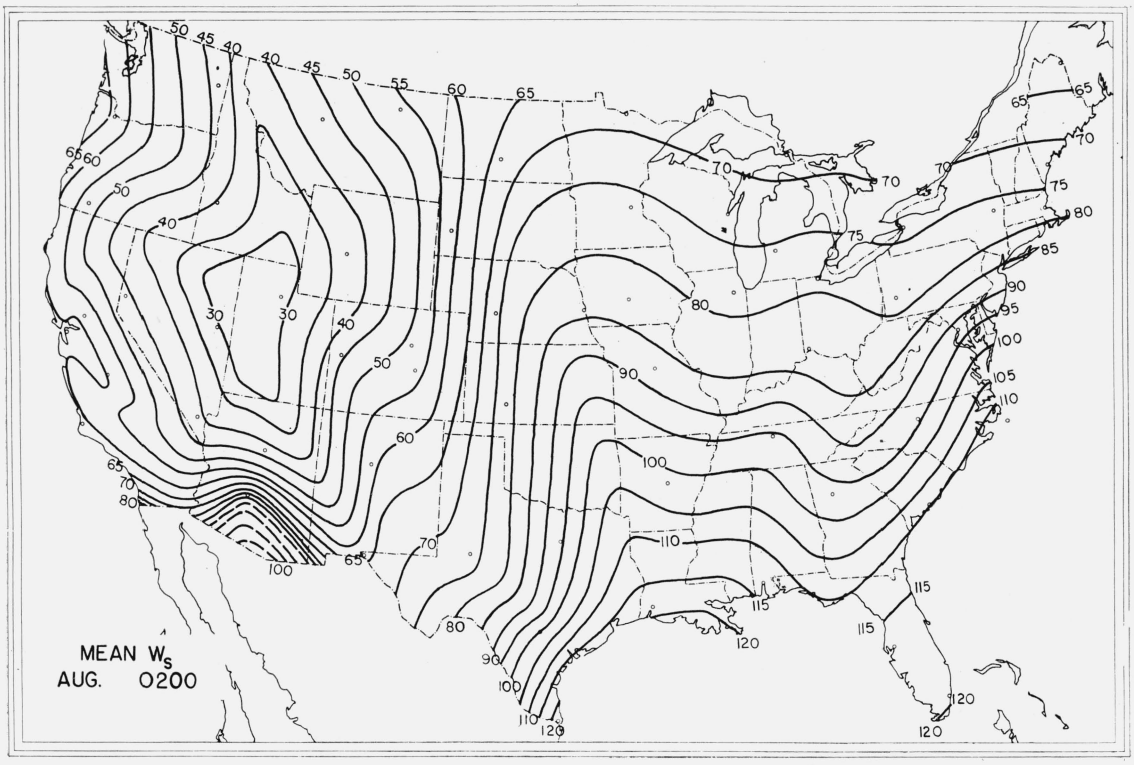

FIGURE 3. *Mean W_s, August 0200 local time.*

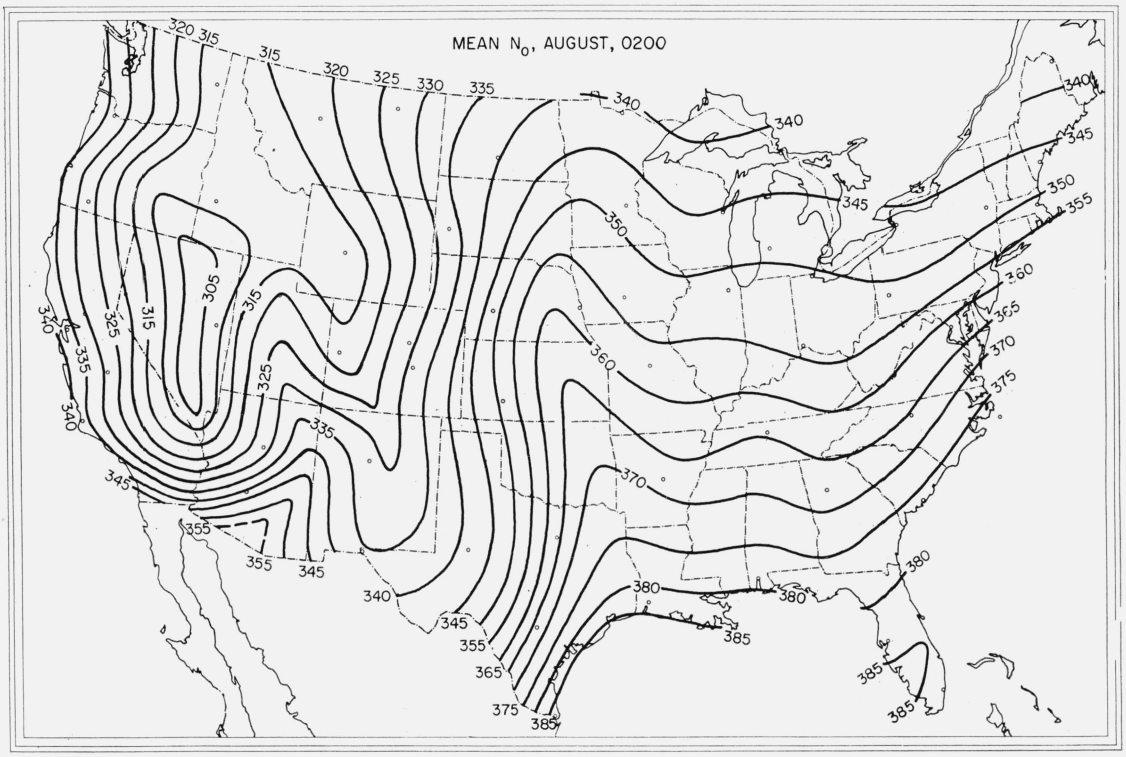

FIGURE 4. *Mean N_o, August 0200 local time.*

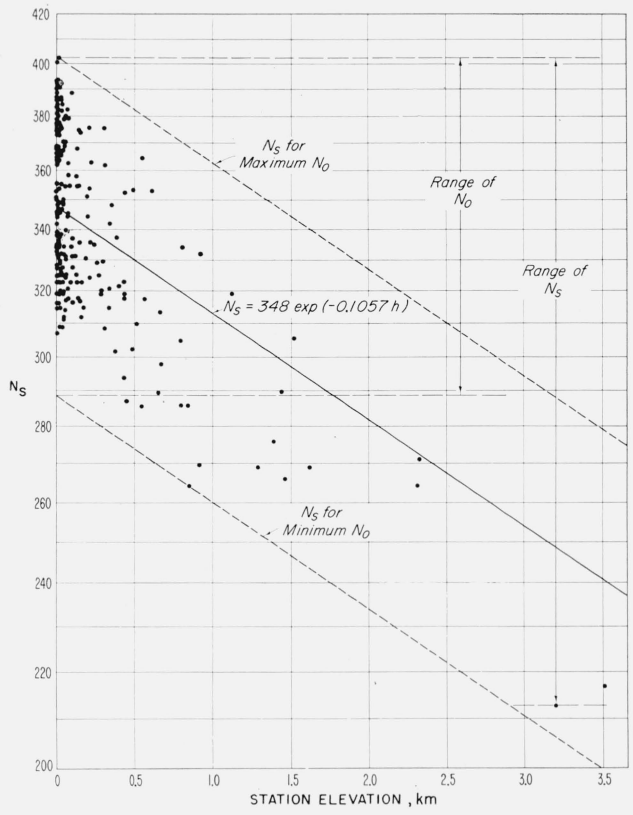

FIGURE 5. *Worldwide values of N_s versus height for August.*

trates the decay of N_s with height for N_0=348. The value of N_s for any other value of N_0 would be obtained from a line parallel to the N_0=348 line but having a zero intercept equal to the new value of N_0. The advantage of adopting N_0 is illustrated by the reduction in range from 190 N units for N_s to 115 N units for N_0, thus diminishing the number of contours of the resulting maps.

It would appear that by removing the influence of station elevation it would be more efficient to estimate N_s from N_0 charts rather than from charts of N_s. As a test of this hypothesis N_s and N_0 contour charts were prepared for both summer and winter from only 42 of the 62 U.S. Weather Bureau stations for which 8-yr means of N_s are available. The remaining 20 stations, distributed at random about the country, were used as a test sample by estimating their 8-yr mean value of N_s from the N_0 and N_s contours. Summertime examples of these charts are given by figures 6 and 7. Note that due to the reduced range of N, the N_0 charts are drawn every 5 N units as compared to the 10-N-unit contours of the N_s charts. The individual deviations of the values obtained from the contour maps with the actual 8-yr means are listed in table 2. By comparing the root mean square (rms) deviations of 10.7 N units in winter and 13.0 N units in summer obtained by estimating N_s from the N_s contours with the 2.7-N-unit rms of estimating N_s from N_0 contours, one concludes that it is at least 4 times more accurate to estimate N_s from N_0 contours than from those of N_s. An inspection of the individual deviations in table 2 indicates that the N_0 contour method is particularly efficient at elevations in excess of 1,200 m or where the terrain is changing rapidly with respect to horizontal distance. As a further practical consequence one notes the remarkable similarity between the N_0 contours of figures 4 and 7, even though the latter contours were derived from only two-thirds of the original data. This indicates that any desired level of accuracy may be maintained with fewer stations (and less expense) by the use of N_0.

TABLE 2.—*Deviations of estimated 8-yr means of* N_s *(calculated from contour charts) from actual 8-yr means for 20 randomly distributed U.S. Weather Bureau stations*

Test station	Height	February 1400			August 0200		
		Actual 8-yr mean value of N_s	Deviation [a]		Actual 8-yr mean value of N_s	Deviation [a]	
			N_s map	N_0 map		N_s map	N_0 map
	Meters	*N units*	*Nunits*	*Nunits*	*N units*	*Nunits*	*Nunits*
Sacramento, Calif.	7	315.6	7.6	0.8	329.6	1.0	−1.8
Portland, Oreg.	8	316.2	4.2	−.5	337.7	19.7	6.0
San Diego, Calif.	11	314.2	−5.8	−2.4	348.1	16.1	3.5
Mobile, Ala.	66	326.6	6.6	4.8	376.0	6.0	0.6
Fresno, Calif.	86	310.6	9.6	3.4	326.2	5.2	4.2
Boston, Mass.	89	308.6	−6.4	−0.5	347.5	−7.5	−0.4
Grand Rapids, Mich.	210	304.4	0.4	−5.9	340.5	−1.5	.1
Columbia, Mo.	239	300.8	−.2	2.4	348.7	−2.3	−2.5
Minneapolis, Minn.	255	301.1	.1	0.6	338.5	−0.5	2.7
Cincinnati, Ohio	271	302.5	−.5	.7	344.1	−2.9	−2.8
Des Moines, Iowa	294	300.9	3.9	2.3	343.1	−1.9	−0.1
Pendleton, Oreg.	455	295.9	1.9	0.4	300.9	2.9	−3.1
Billings, Mont.	1,088	269.3	−2.3	.1	285.6	5.6	1.2
Burns, Oreg.	1,262	268.1	−23.9	−3.2	271.3	−15.7	−4.4
Salt Lake City, Utah	1,288	266.3	1.3	−0.8	279.5	8.5	4.4
Reno, Nev.	1,340	259.6	−20.4	−6.8	277.6	−29.4	1.6
Pocatello, Idaho	1,355	264.7	−2.3	0.4	269.7	−3.3	0.0
Denver, Colo.	1,625	244.9	−8.1	.7	276.6	−1.4	.3
Colorado Springs, Colo.	1,882	237.1	−15.9	−.6	272.4	−6.6	1.1
Flagstaff, Ariz.	2,131	237.8	−26.2	2.3	261.4	−36.6	−2.2
Root mean square deviation			10.7	2.7		13.0	2.7

[a] Deviation equals the actual long-term mean minus the value obtained from map contours.

3. Worldwide Values of N_0

Mean values of N_0 were calculated at each of the 306 selected stations and charts were prepared for each month of the year. The charts for February and August are given on figures 8 and 9. It is seen that the values of N_0 for sea-level stations vary from 390 in the maritime tropical areas to 290 in the deserts and high plateaus. The interior of continents and mountain chains in middle latitudes are reflected by low values as compared to those of coastal areas. Further, such pronounced climatic details as the Indian monsoon and the effects of coastal mountain ranges blocking prevailing winds and producing rain shadows are indicated by these N_0 contours.

The annual variation of N_s is indicated on figure 10 by contours of the difference between the maximum and minimum monthly means observed throughout the year. It is quite remarkable how clearly climatic differences are evidenced by the

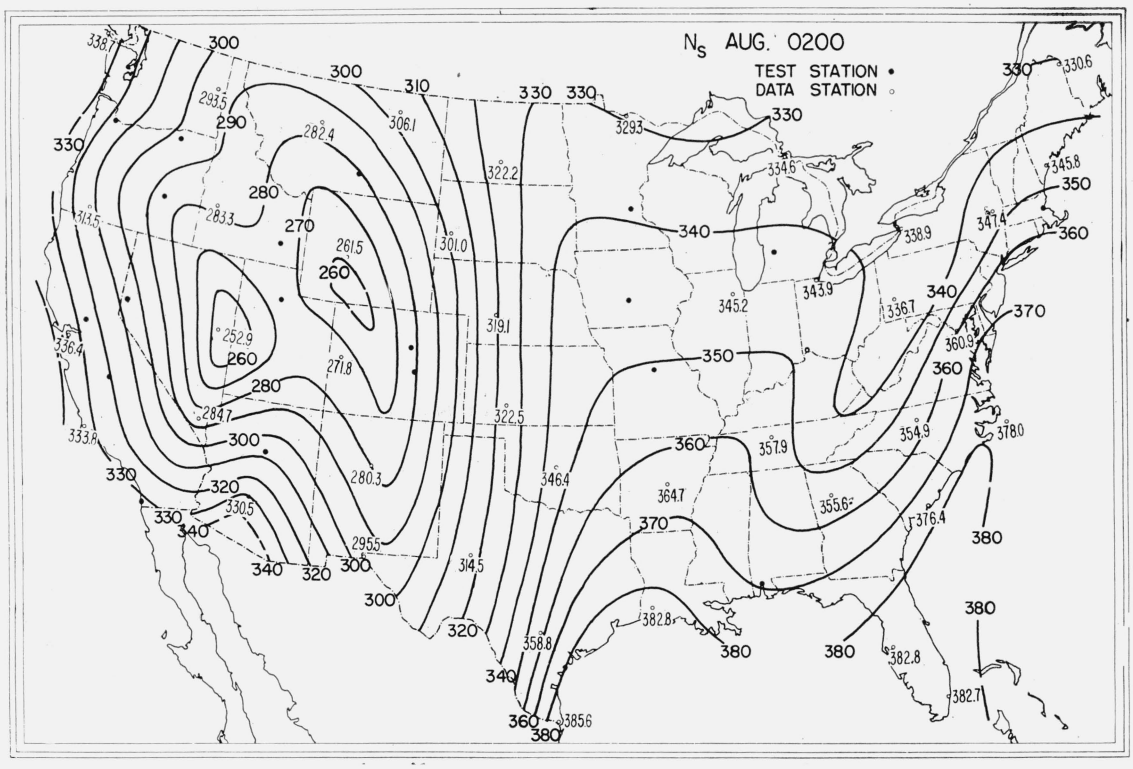

FIGURE 6. *Test chart of mean N_s August 0200 local time.*

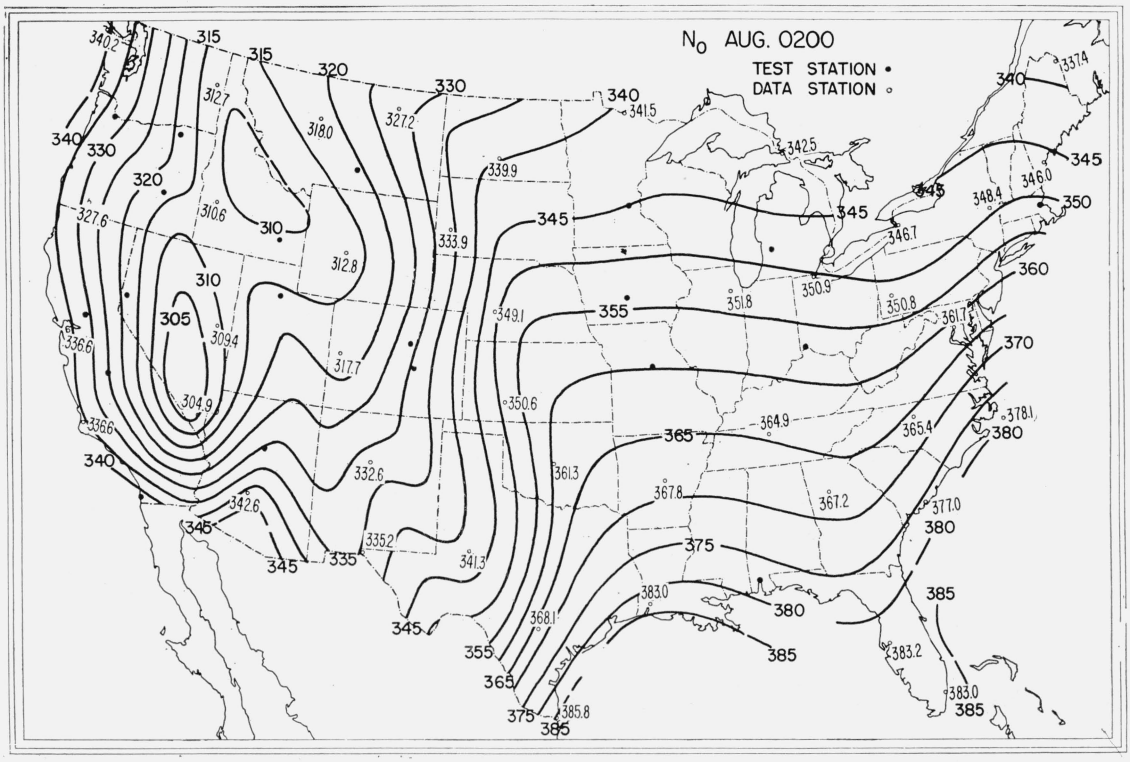

FIGURE 7. *Test chart of mean N_o August 0200 local time.*

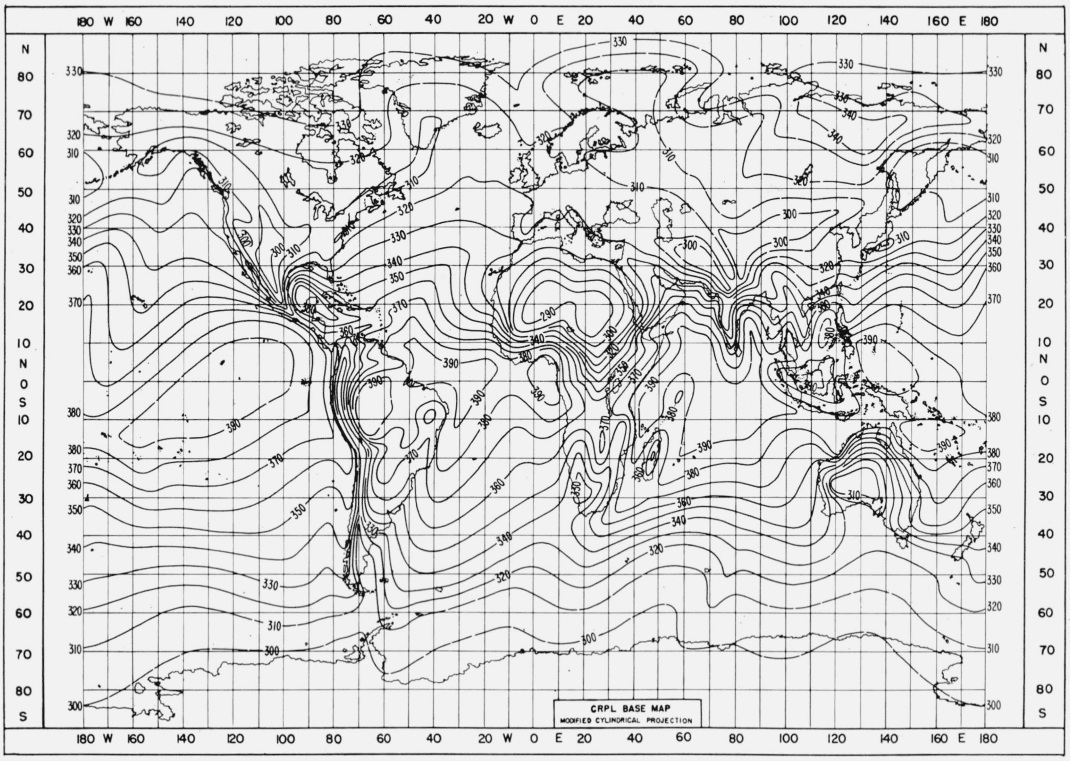

FIGURE 8. *Worldwide values of mean N_o for February.*

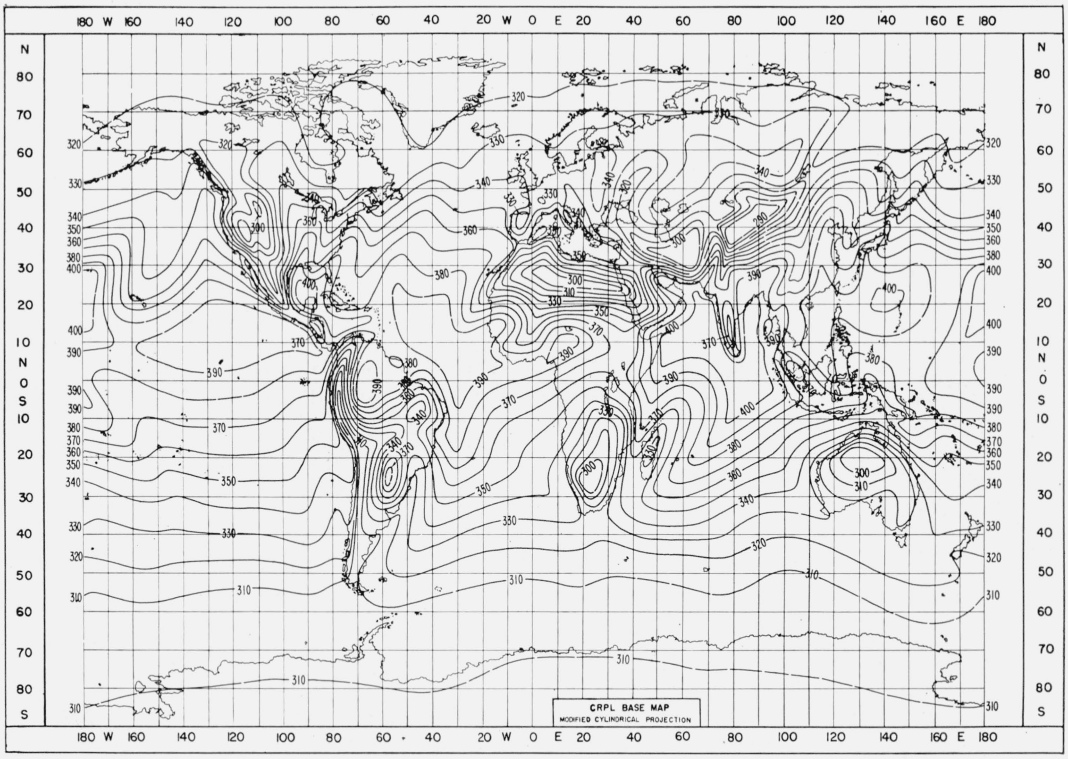

FIGURE 9. *Worldwide values of mean N_o for August.*

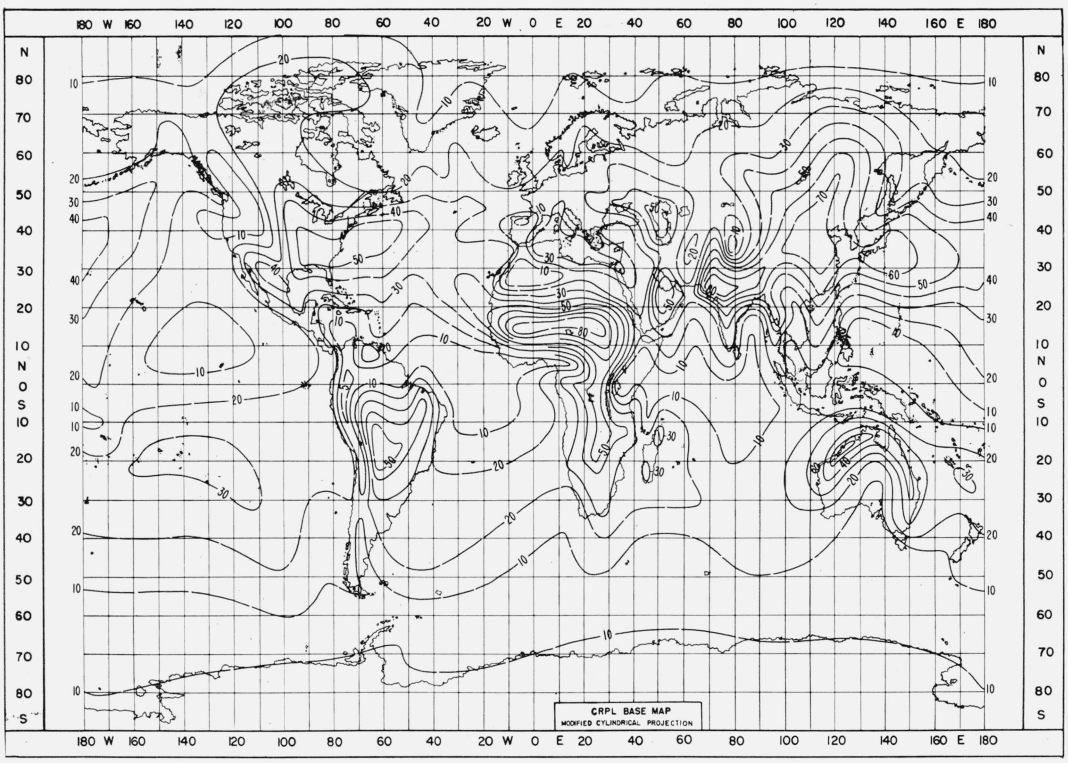

FIGURE 10. *Annual range of monthly mean N_s.*

yearly range of N_s. The prevailing transport of moist maritime air inland over the west coasts of North America and Europe is indicated by relatively small annual ranges (20 to 30 N units), while, for example, the east coast of the United States with a range of 40 to 50 N units or more reflects the invasion of that area from time to time by such diverse air-masses as arctic continental and tropical maritime. The largest annual ranges of N_s (90 N units) are observed in the Sudan of Africa and in connection with the Indian monsoon.

An additional N_0 map (fig. 11) was prepared from the minimum monthly mean value of N_s observed throughout the year to supplement the range map in order that an estimation might be made of both the minimum and maximum monthly mean N_s expected during the year.

A measure of the variability of the February and August mean values of N_s is given by monthly range maps (fig. 12 and 13) determined from monthly averages from 5 yr of data. Ranges are given by the maximum difference of the five individual monthly mean values. In contouring the two variability maps only those terrestrial regions having reasonable data coverage are included. Dashed contours are shown for areas of sparse or unreliable data. The general picture of the worldwide distribution of N_s variability is that of a number of continentally located cells of moderate range accompanied by somewhat random small-scale variations over ocean areas. Regions of large range, from 40 to as much as 70 N units, are present, however, in Australia and on islands of the adjoining oceans, on the African equatorial plateau near the Cameroons and in the Great Basin of the southwestern United States. Common to all these areas of large year-to-year variability, at least during the summer season, are high mean temperatures ranging from about 25° to 30° C, the variability being due to relatively small variations of humidity. It is felt that when a more dense network of stations is available for a longer period of record, say 10 yr, areas of high monthly variability are likely to be more extensive in tropical and desert areas than indicated on our present maps.

4. Climatic Classification by N_s

The annual cycle of N_s at each station was examined for the purpose of deriving similarities of climatic pattern. As one form of climatic classification, the annual mean value of N_s at each station was plotted versus the annual range at the station. When this was done, several distinct groupings of data seemed evident. These groupings, described in table 3, are intended to give a general idea of the geographic and climatic character of the majority of the stations found within given values of range and yearly mean of N_s.

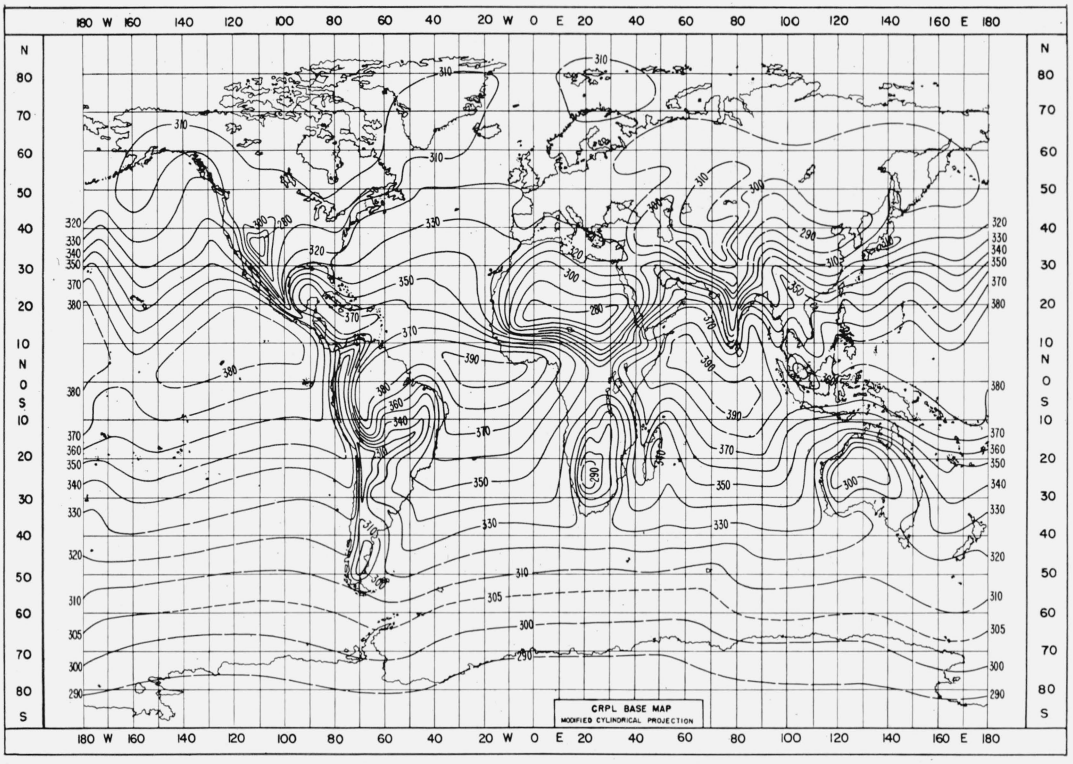

FIGURE 11. *Minimum monthly mean value of* N_a.

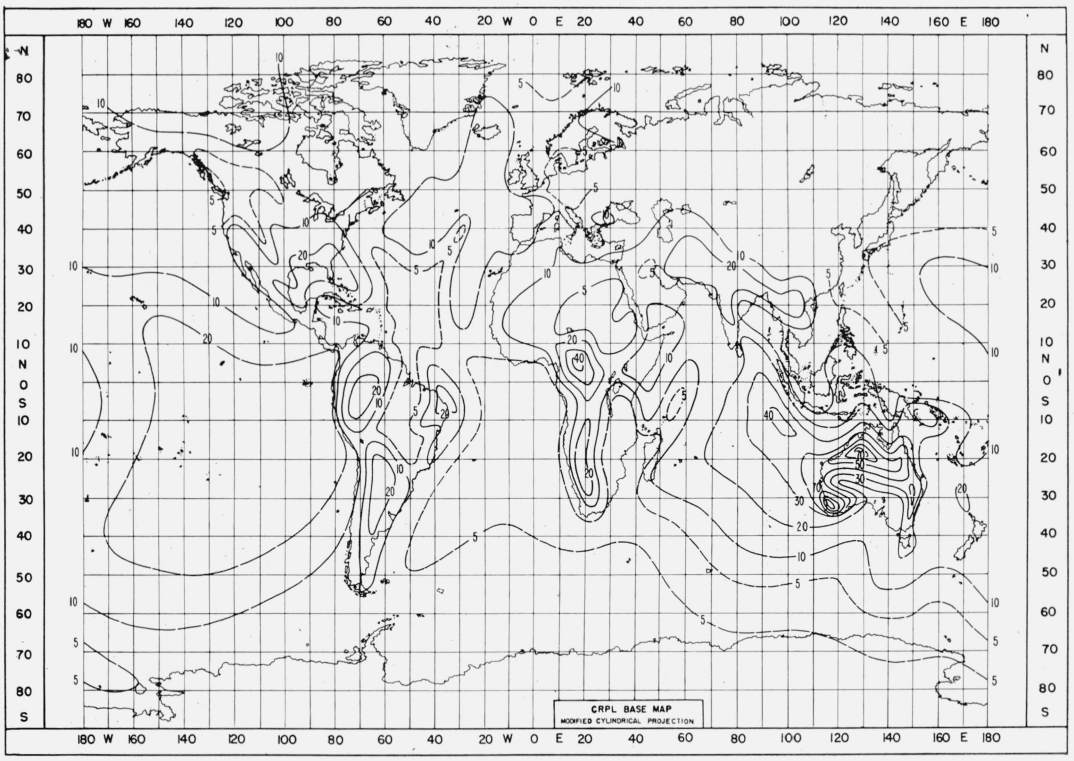

FIGURE 12. *Year-to-year range of monthly mean* N_s *for February.*

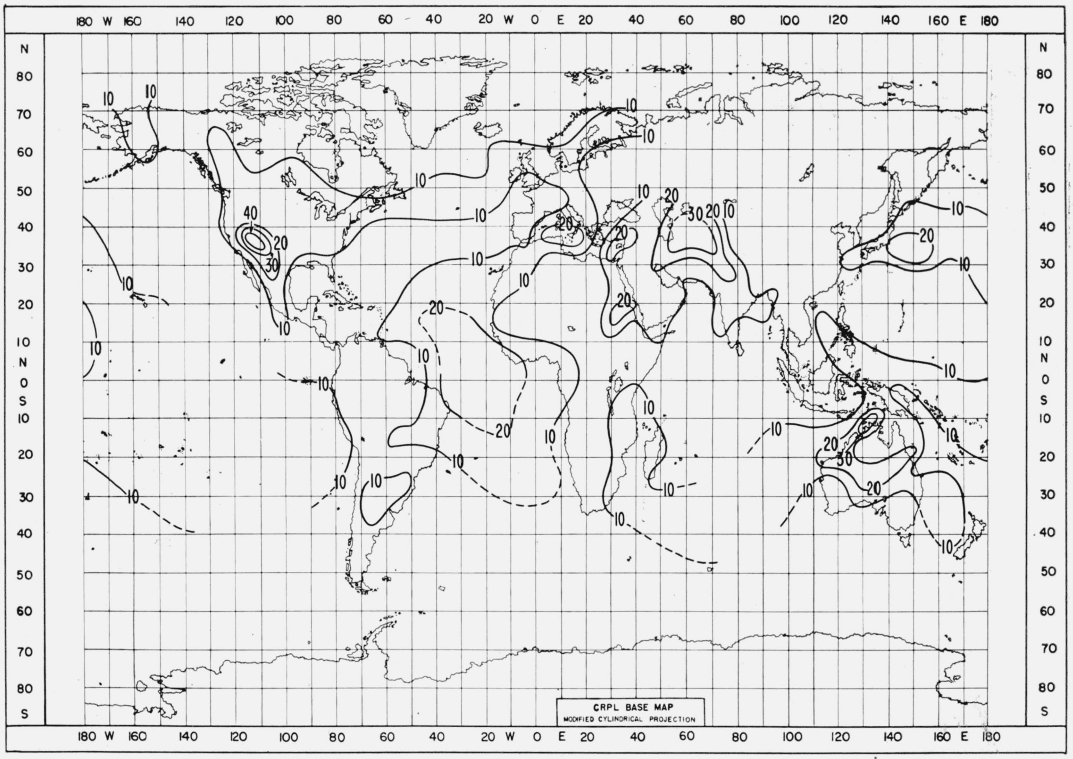

FIGURE 13. *Year-to-year range of monthly mean N_s for August.*

TABLE 3. *Characteristics of climatic types*

Type	Location	Annual mean N_s	Annual range of N_s	Characteristics
		N units	*N units*	
I Midlatitude-coastal	Near the sea or in lowlands on lakes and rivers, in latitude belts between 20° and 50°.	300 to 350	30 to 60	Generally subtropical with marine or modified marine climate.
II Subtropical-Savanna	Lowland stations between 30° N and 25° S lat., rarely far from the ocean.	350 to 400	30 to 60	Definite rainy and dry seasons, typical of Savanna climate.
III Monsoon-Sudan	Monsoon—generally between 20° and 40° N lat., Sudan—across central Africa from 10° to 20° N lat.	280 to 400	60 to 100	Seasonal extremes of rainfall and temperature.
IV Semiarid-mountain	In desert and high steppe regions as well as mountainous regions above 3,000 ft.	240 to 300	0 to 60	Year-round dry climate.
V Continental-Polar	In middle latitudes and polar regions. (Mediterranean climates are included because of the low range resulting from characteristic dry summers.)	300 to 340	0 to 30	Moderate or low annual mean temperatures.
VI Isothermal-equatorial	Tropical stations at low elevations between 20° N and 20° S lat., almost exclusively along seacoasts or on islands.	340 to 400	0 to 30	Monotonous rainy climates.

For a given classification of refractive-index climate, diverse meteorological climates and geographical regions may be represented. Note, for example, that type V of table 3 includes stations from Mediterranean and marine as well as polar climates. Mediterranean stations in this category fail to attain a high range because of the characteristic dryness of the subtropical high-pressure pattern that is generally found in this area during the summer months. Polar and marine climates in this group maintain a low range due to suppressed humidity effects as a result of low to moderate year-around average temperatures.

Annual trends of N_s for stations typical of each climatic division are shown by figure 14.

Yet another facet of the climate is the year-to-year variation of the monthly mean value of N_s. Five consecutive years of monthly means were prepared for each of the six typical stations whose annual cycles are shown in figure 14. Then, for each month, the absolute value of the difference between consecutive years was obtained. These values were then averaged for all months and are listed in the second column of table 4.

Another measure of the variation of monthly mean values of N_s is obtained by differencing the maximum and minimum values occurring for a given month during the 5-yr period. These differences are also given in table 4 for the months of February, May, August, and November.

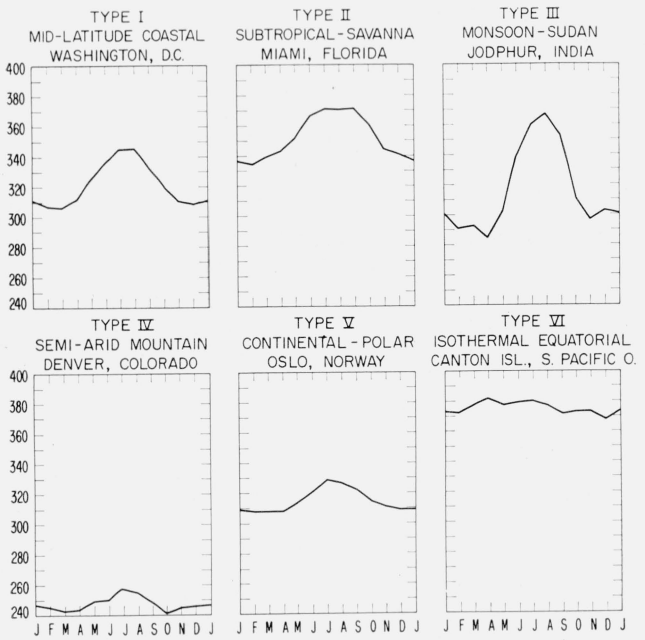

FIGURE 14. *Representative annual cycles of N_s for the major climatic types.*

TABLE 4. *Year-to-year differences of monthly mean N_s*

Climatic type	Difference between monthly means in successive years for the same month, averaged for all seasons over a 5-yr period	Maximum differences between monthly means over a 5-yr period			
		Feb.	May	Aug.	Nov.
I	5.7	6.0	16.5	17.0	7.0
II	5.4	8.5	6.5	8.0	11.0
III	8.9	16.5	14.5	20.0	6.5
IV	5.4	10.5	11.5	13.5	6.5
V	4.7	5.5	11.5	10.0	5.0
VI	7.1	9.5	25.5	8.5	8.5

5. Applications

The communications engineer usually has available a small amount of measured field strength data from limited tests of a particular system. He must then estimate the expected signal level or practical range of that system, or other systems, for other times of the year, other years and in other areas. The variation of signal level from month to month and climate to climate can be explained, in part, by its observed correlation with N_s.

Pickard and Stetson [8, 9] were among the first to note the correlation of N_s and received field strengths. The correlation of N_s and field strength over a particular path has been studied quantitatively [10, 11] and found to be highest (correlation coefficients of 0.8 to 0.95) when the variables are averaged over periods of a week to a month. This latter study has shown that the regression coefficient (decibel change in field strength per unit change in N_s) varies diurnally from 0.14 db in the afternoon hours to 0.24 db per unit change of N_s in the early morning hours. This correlation is so sufficiently consistent that Gray [12] and Norton [13] have utilized it in their recent prediction methods of transmission loss in a band from 100 to 50,000 Mc. In addition, the coefficient 0.2 db per unit change in N_s has been tentatively adopted by CCIR Study Group V in their revision of the 30- to 300-Mc tropospheric-wave propagation curves to account for the geographic and seasonal variations of field strengths. The estimates of field strength variations attributed to N_s given below are based upon the CCIR coefficient.

If one assumes, for comparison only, that the worldwide average value of N_s is 330 and that one is able to estimate the field strength level of a particular communications system at a given distance and for $N_s=330$, then the above correlations would indicate that the climatic variations of fields given in table 5 might be expected.

TABLE 5.—*Climatic variation of hypothetical communications system relative to predicted value for $N_s=330$, assuming a 0.2-db variation per unit change in N_s*

Climatic type [a]	Expected yearly mean field strength level relative to $N_s=330$	Expected annual range on the above assumption
	db	*db*
I	−6 to +4	6 to 12
II	+4 to +14	6 to 12
III	−10 to +14	12 to 20
IV	−18 to −6	0 to 12
V	−6 to +2	0 to 6
VI	+2 to +14	0 to 6

[a] Climatic types are the same as those in table 3.

The data of table 5 indicate, for example, that identically equipped tropospheric communications systems could display as much as a 32-db difference in mean signal-strength level due to the climatic difference of say, Denver, Colorado and the tropics. Further one might expect the monthly mean field strength of this hypothetical system to vary throughout the year from less than 12 db in the high plains near Denver to as much as 20 db in the African Sudan.

Under this same assumption, figures 10 and 11 allow the communications engineer to estimate the expected maximum and minimum monthly mean field strength expected throughout the year.

The year-to-year variations of the monthly mean N_s listed in table 4 indicate that the monthly mean of field strength for a particular month may differ in successive years by as little as 1.0 db for climatic category V in November or as much as 5.1 db for category VI in May.

Another application of these worldwide charts is to aid in estimating the refraction of radio waves. The most convenient method of accounting for the effects of atmospheric refraction is by means of the effective-earth's-radius concept of Schelling, Burrows, and Ferrel [14]. The effective earth's radius, a_e, is determined from

$$a_e=\left(\frac{1}{1+\frac{a}{n}\frac{dn}{dh}}\right)a, \qquad (6)$$

where a is the true radius of the earth, n is the refractive index, and dn/dh is the initial n gradient with respect to height. A great simplification of propagation calculations is accomplished by assuming that dn/dh is a constant, thus allowing radio rays to be drawn as straight rays over a fictitious earth of radius a_e rather than curved rays over the true earth of radius a. This simplification allows, for example, the distance to the radio horizon, d, of a radio ray leaving an antenna of height, h, to be calculated from

$$d=\sqrt{2a_eh}. \tag{7}$$

One notes, however, that the determination of a_e involves dn/dh as well as n and that our N_0 charts allow only an estimation of n. This disparity may be resolved by utilizing the observation that N_s is highly correlated with the value of N at 1 km above the surface. The difference between N_s and N at 1 km is denoted ΔN. It has been noted [15] that the correlation coefficient between ln $|\Delta N|$ and N_s is 0.926 for 888 sets of data from 45 U.S. weather stations representing many diverse climates. The regression equation

$$-\overline{\Delta N}=7.32\ \exp\{0.005577\ \overline{N_s}\} \tag{8}$$

results when both variables are averaged over 6 to 8 yr of record. Approximating dn/dh in (6) by ΔN we may determine that the radio horizon distance of an antenna located 150 m above the earth would vary from 48 km when $N_s=200$ to 59 km when $N_s=400$. Yet another application of the N_s charts is to the exponential models of the decrease of refractive index with height which have been recently proposed [15, 16]. These models are completely specified by N_s and may be used to account for seasonal and geographic variations of such refraction effects as radar range and elevation angle errors.

6. Critical Appraisal of Results

The world maps presented above were based upon data from 306 weather stations. This number of stations appears to be consistent with the scale of map used. The map scale is so small, however, that only large climatic differences can be expected to be discerned. For the climate of any given area one should refer to detailed studies of N such as those currently in preparation for the United States at the Central Radio Propagation Laboratory.

The accuracy of the present charts may be assessed from the charts of maximum range, R, of monthly means as given by figures 12 and 13. The standard deviation of the individual monthly means may be estimated from [17], 0.43 R, where the coefficient 0.43 is appropriate for five individual observations. Since, in general, $R\leq 20$ N units, then 0.43 $R\leq 9N$ units, although this standard deviation may be as large as 26 N units for the month of February in Australia and 17 N units in the southwest of the United States during August, or in the African Sudan during February.

Further, the standard error of estimating a five year mean from five individual monthly values is determined from

$$\frac{0.43\ R}{\sqrt{n}},$$

where n for our case is 5 and thus the error of the 5 yr mean would be 0.192 R. Remembering that $R\leq 20$ N units and assuming perfect skill in drawing the contours, one would expect the standard error of estimate to be less than 4 N units. This standard error can be as large as 12 N units in Australia where $R=60$ N units.

The value of N_s at each of the 20 test stations of section 2 was estimated from the N_0 contours with an rms error of 5 N units which is consistent with the standard error of estimate obtained from the range charts. In the large areas of sparse data, such as the oceans and Russia, this uncertainty rises to about 10 N units and thus the contours in these regions are dashed.

At the time the present study was initiated it was felt that N_s should be reduced to sea level by at least the dry term correction factor as in eq (5). The absence of published work on models of N structure in the free atmosphere encouraged the decision to rest on prudence and adopt this dry term correction factor. Since that time several effective exponential models of the free atmosphere have been demonstrated [15, 16] and it now appears that it might be better in future work to use the slightly larger exponential coefficient which corresponds to the decay of N in the free atmosphere. If the free atmosphere decay were adopted, then the range of N_0 values on the world maps would be reduced from 115 to 110 N units, i.e., less than 5 percent. Since this reduction in range is an order of magnitude less than the original reduction accomplished by the use of N_0, it appears that the basic advantage of the adoption of the concept of a reduced value has been realized with the initial correction. To produce a significantly large reduction in the range of the present map contours it would appear that the seasonal and diurnal variation of the exponential coefficient would have to be considered; a process which appears at present to be unduly complex.

7. Conclusions

With the above critical appraisal in mind, the salient conclusions of the present study are:

(a) The radio refractive index varies in a systematic fashion with climate, and different climates may be indentified by the range and mean values of the refractive index.

(b) It is 4 or 5 times more accurate to estimate the station value of the index from charts of the reduced-to-sea-level index than from charts of the station value. This improved accuracy results from using a method that allows height dependence to be accurately taken into account.

(c) Identically equipped tropospheric communications might be expected to vary as much as 30 db in monthly mean signal level in different climatic regions, and the annual range of monthly mean field strength could be as high as 20 db in the Sudan of Africa and as low as 0 to 6 db in the high plains of the western United States.

The authors express their appreciation to Mrs. G. E. Richmond, Mrs. P. C. Whittaker, and Mrs. M. F. Fischer for their aid in the preparation of the basic data, to A. M. Ozanich for cartographic assistance, and to Miss G. Hoffmire for preparation of the manuscript.

8. References

[1] E. K. Smith, Jr. and S. Weintraub, The constants in the equation for atmospheric refractive index at radio frequencies, Proc. IRE **41,** 1035 (1953).
[2] IMO list of Resolutions of the Conference of Directors, Washington, 22d Sept.–11th Oct. 1947, Lausanne, 1948, Resolution No. 71 [CCI Toronto 1947: XIII].
[3] World atlas of sea surface temperatures, Hydrographic Office Publication No. 225, 2d Ed. 1944, Washington, D.C.
[4] Atlas of climatic charts of the oceans, U.S. Weather Bureau Publication No. 1247 (Washington, D.C., 1938).
[5] W. E. Johnson, An analogue computer for the solution of the radio refractive-index equation, J. Research NBS **51,** 335 (1952) RP2462.
[6] B. Haurwitz, Dynamic meteorology, p. 11–12 (McGraw-Hill Book Co., New York, N.Y., 1941).
[7] Smithsonian Meteorological Tables, Table 63, Sixth Revised Ed. (Washington, D.C., 1951).
[8] G. W. Pickard and H. T. Stetson, Comparison of tropospheric reception, J. Atmospheric and Terrest. Phys. **1,** 32 (1950).
[9] G. W. Pickard and H. T. Stetson, Comparison of tropospheric reception at 44.1 Mc with 92.1 Mc over the 167-mile path of Alpine, N.J. to Needham, Mass., Proc. IRE **38,** 1450 (1950).
[10] B. R. Bean, Some meteorological effects on scattered radio waves, IRE Trans. **PGCS–4** 32 (1956).
[11] M. Onoe, M. Hirai, and S. Niwa, Results of experiment of long-distance overland propagation of ultra-short waves, J. Radio Research Labs. (Japan) **5,** 79 (1958).
[12] R. E. Gray, The refractive index of the atmosphere as a factor in tropospheric propagation far beyond the horizon, IRE National Conv. Record, **Pt 1,** 3 (1957).
[13] K. A. Norton, Point-to-point radio relaying via the scatter mode of trophospheric propagation, IRE Trans. **PGCS–4,** 39 (1956).
[14] J. C. Schelling, C. R. Burrows, and E. B. Ferrell, Ultra-Short-Wave Propagation, Proc. IRE **21,** 427 (1933).
[15] B. R. Bean and G. D. Thayer, On models of the atmospheric refractive index, Proc. IRE **47,** 740 (1959).
[16] L. J. Anderson, Tropospheric bending of radio waves, Trans. Am. Geophys. Union **39** 208 (1958).
[17] G. W. Snedecor, Statistical methods, 4th ed., p. 97–98 (Iowa State College Press, Ames, Iowa, 1946).

Boulder, Colo. (Paper 63D3–22)